Gadolinium Chelate Contrast Material in Pregnancy: Fetal Biodistribution in the Nonhuman Primate[1]

Karen Y. Oh, MD
Victoria H. J. Roberts, PhD
Matthias C. Schabel, PhD
Kevin L. Grove, PhD
Mark Woods, PhD
Antonio E. Frias, MD

Purpose: To determine the extent to which gadolinium chelate is found in nonhuman primate fetal tissues and amniotic fluid at 19–45 hours after intravenous injection of a weight-appropriate maternal dose of the contrast agent gadoteridol.

Materials and Methods: Gravid Japanese macaques (n = 14) were maintained as approved by the institutional animal care and utilization committee. In the 3rd trimester of pregnancy, the macaques were injected with gadoteridol (0.1 mmol per kilogram of maternal weight). Fetuses were delivered by means of cesarean section within 24 hours of maternal injection (range, 19–21 hours; n = 11) or 45 hours after injection (n = 3). Gadolinium chelate levels in the placenta, fetal tissues, and amniotic fluid were obtained by using inductively coupled plasma mass spectrometry. The Wilcoxon rank sum test was used for quantitative comparisons.

Results: Gadoteridol was present in the fetoplacental circulation at much lower quantities than in the mother. At both time points, the distribution of gadolinium chelate in the fetus was comparable to that expected in an adult. The highest concentration of the injected dose (ID) was found in the fetal kidney (0.0161% ID per gram in the 19–21-hour group). The majority of the in utero gadolinium chelate was found in the amniotic fluid and the placenta (mean, 0.1361% ID per organ ± 0.076 [standard deviation] and 0.0939% ID per organ ± 0.0494, respectively). Data acquired 45 hours after injection showed a significant decrease in the gadolinium chelate concentration in amniotic fluid compared with that in the 19–21-hour group (from 0.0017% to 0.0007% ID per gram; P = .01).

Conclusion: Amounts of gadolinium chelate in the fetal tissues and amniotic fluid were minimal compared with the maternal ID. This may impact future clinical studies on the safety of gadolinium contrast agent use in pregnancy.

[1] From the Department of Radiology (K.Y.O.), Advanced Imaging Research Center (M.C.S., M.W.), and Department of Obstetrics and Gynecology, Division of Maternal Fetal Medicine (A.E.F.), Oregon Health and Science University, 3181 SW Sam Jackson Park Rd, MC L340, Portland, OR 97239; Division of Diabetes, Obesity and Metabolism, Oregon National Primate Research Center, Oregon Health and Science University, Beaverton, Ore (V.H.J.R., K.L.G., A.E.F.); and Department of Chemistry, Portland State University, Portland, Ore (M.W.). Received June 24, 2014; revision requested August 21; revision received November 5; accepted December 5; final version accepted December 18. **Address correspondence to** K.Y.O. (e-mail: *ohk@ohsu.edu*).

Traditionally, fetal and placental imaging has been centered on ultrasonography (US), which is considered safe in pregnancy and can provide excellent anatomic resolution of the developing fetus and placenta. Similar to US in nongravid patients, limitations include patient-dependent resolution and lack of ability to obtain functional data. Magnetic resonance (MR) imaging allows non–contrast material–enhanced imaging of the fetus and placenta for detailed evaluation of the anatomy and is being studied for use in advanced fetal applications, including gated fetal cardiac imaging and the assessment of placental function and fetal structural brain development (1–3). When imaging the morbidly adherent placenta with MR imaging, gadolinium chelate use is controversial but may increase specificity and be valuable for assessing the degree of placental invasion (4–8). With the growing use of MR imaging for various disease processes, protocols that would otherwise utilize contrast material are often altered for the incidentally pregnant patient (9,10).

Advances in Knowledge

- After intravenous injection of gadoteridol into a pregnant nonhuman primate, there is evidence of transplacental passage of gadolinium chelate into the fetal circulation, although the majority of the contrast agent dose remains in the maternal circulation.
- The highest concentration of the injected dose (ID) was found in the fetal kidney (0.0161% ID per gram in the 19–21-hour group).
- The majority of the in utero gadolinium chelate was found in the amniotic fluid and the placenta (0.1361% ID per organ ± 0.076 [standard deviation] and 0.0939% ID per organ ± 0.0494, respectively).
- Minimal gadolinium chelate is detected in the fetal tissues at 21 and 45 hours after maternal contrast agent injection.

Gadolinium (Gd^{3+}) chelates are traditionally avoided in pregnancy because of potential safety concerns for the fetus and are listed as a Class C drug by the U.S. Food and Drug Administration. In general, Class C drugs should be used only if the potential benefits outweigh the potential risks to the fetus (11,12). The European Society of Urogenital Radiology Contrast Media Safety Committee guidelines state that the highest-risk gadolinium contrast media are contraindicated in pregnant women, while the intermediate- and lowest-risk gadolinium contrast media may be given to pregnant women in the lowest dose required to provide essential diagnostic information (12).

Understanding the physiology of gadolinium chelate distribution in the fetus is the basis for assessing safety in pregnancy. In animal models, including mice, rats, and rabbits, gadolinium-based contrast medium has been injected intravenously into the pregnant animal at high doses, showing that gadolinium chelate reaches the fetal circulation (13–15). Gadolinium-based contrast material crosses the placenta into the fetal circulation, to be excreted by the fetal kidneys into the amniotic fluid (13,15,16). In nonhuman primates, gadolinium chelate has been found to enhance the placenta and has subsequently been seen in the fetal bladder on serial MR image acquisitions (16). However, to our knowledge, the quantitative levels of Gd^{3+} in the primate fetus have not previously been measured.

The effect of gadolinium-based contrast material on the developing fetus is unknown. Defining the levels of Gd^{3+} in the fetal environment after maternal intravenous injection would be the first step in evaluating any potential effect on the fetus. The aim of this study was to determine the amount of Gd^{3+} in the nonhuman primate fetus and amniotic fluid at 19–21 and 45 hours after administration of a maternal intravenous dose of 0.1 mmol per kilogram of body weight of a gadolinium-based contrast agent, gadoteridol (ProHance; Bracco Diagnostics, Princeton, NJ).

Implication for Patient Care

- Among animal models, placental organization in nonhuman primates is most similar to that of the human placenta; we report the gadolinium chelate levels in nonhuman primate fetuses after maternal gadoteridol injection, and therefore our results may have implications for the safety of contrast-enhanced MR imaging during pregnancy.

Materials and Methods

Animals

All protocols were prospectively approved by the Institutional Animal Care and Utilization Committee of the Oregon National Primate Research Center, and guidelines for humane animal care were followed.

Study animals were part of an existing study of the use of dynamic contrast-enhanced MR imaging to evaluate primate placental vascular organization (3,17). The dynamic contrast-enhanced MR imaging study is part of an ongoing nonhuman primate model developed to demonstrate that consumption of a

Published online before print
10.1148/radiol.15141488 **Content code:** OB

Radiology 2015; 276:110–118

Abbreviations:
ID = injected dose
ROI = region of interest

Author contributions:
Guarantors of integrity of entire study, K.Y.O., A.E.F.; study concepts/study design or data acquisition or data analysis/interpretation, all authors; manuscript drafting or manuscript revision for important intellectual content, all authors; manuscript final version approval, all authors; agrees to ensure any questions related to the work are appropriately resolved, all authors; literature research, K.Y.O., V.H.J.R., A.E.F.; experimental studies, V.H.J.R., M.C.S., K.L.G., M.W., A.E.F.; statistical analysis, M.C.S.; and manuscript editing, K.Y.O., V.H.J.R., M.C.S., M.W., A.E.F.

Funding:
This research was supported by the National Institutes of Health (grants R21-HD-076265, R24-DK-090964, P51-OD-011092, S10RR025512-01, and P30 CA69533).

Conflicts of interest are listed at the end of this article.

Western-style diet, independent of maternal obesity and/or diabetes, causes broad developmental issues in the fetus and that placental dysfunction, abnormal uterine hemodynamics, and placental inflammation are important contributors to these developmental abnormalities (17–27). Japanese macaques (n = 9) were maintained on a high-fat diet (36% calories from fat, Test Diet, 5 L0P; Purina Mills, Richmond, Ind) supplemented with calorically dense treats for 4–7 years. The composition of the high-fat diet represents a typical Western-style diet in regard to the saturated fat content. Control animals (n = 5) were fed standard chow, which provides 14% calories from fat. All animals were socially housed in indoor-outdoor pens with one or two male macaques and three to 11 female macaques per diet-determined cohort and had ad libitum access to food and water. Animals were allowed to breed naturally, and pregnancies were identified by means of routine US.

Term pregnancy for macaques is approximately 175 days. Delivery at gestational day 130 (equivalent to the 3rd trimester) was planned for all pregnant macaques undergoing dynamic contrast-enhanced MR imaging. For the purposes of this study, two time points after maternal dosing were used. In the 19–21-hour group, dynamic contrast-enhanced MR imaging was performed at gestational day 129 (n = 11, with three control animals and eight animals receiving the high-fat diet). In the 45-hour group, dynamic contrast-enhanced MR imaging was performed at gestational day 128 (n = 3, with two control animals and one animal receiving the high-fat diet). A total of 14 pregnant macaques and their fetuses were evaluated for this study. All 14 animals underwent dynamic contrast-enhanced MR imaging for the purposes of the primary existing study protocol for placental evaluation (3).

After an overnight fast, animals were initially sedated with 3–5 mg/kg intramuscular Telazol in preparation for the MR imaging protocol, which included gadoteridol injection. Once intubated, the macaque was maintained in a state of general anesthesia with 1%–2% isoflurane gas. Flumazenil (0.01 mg/kg) was administered intravenously to reverse the effects of Telazol (3).

Gadolinium Chelate Injection

Gadoteridol (ProHance) was injected intravenously into the cephalic vein of the sedated gravid macaque during dynamic contrast-enhanced MR imaging (study and data reported separately [3]). Gadoteridol is the chelate formed between Gd^{3+} and 10-(2-hydroxypropyl)-1,4,7,10-tetraazacyclododecane-1,4,7-triacetate. The dose of gadoteridol was based on a standard clinical dose of 0.1 mmol per kilogram of maternal weight. Maternal weight ranged from 8.1 to 17.8 kg, with a mean of 12.6 kg. Animals underwent dynamic contrast-enhanced MR imaging series of T1-weighted three-dimensional gradient-recalled-echo sequences in a Siemens (Erlangen, Germany) whole-body 3.0-T MR imaging system, with a CP transmit 15-channel receive radiofrequency coil (QED, Cleveland, Ohio) (3).

Tissue Collection

Fetuses were delivered by cesarean section and were taken immediately to the pathology unit for full necropsy. Placenta, amniotic fluid, and fetal tissues were harvested, dissected, and snap frozen in liquid nitrogen. Fetal tissue samples included brain, liver, and kidney samples from all 14 fetuses. Fetal skin samples were obtained from three fetuses in the 19–21-hour group, and bone samples (from the femur or calvarium) were obtained from three fetuses in the 19–21-hour group. Skin and bone samples were not obtained from all fetuses because these tissues were not harvested initially as part of the existing placental dynamic contrast-enhanced MR imaging study protocol. Maternal plasma samples were collected, processed, and stored at –80°C for later analysis.

In Vivo Gd^{3+} Analysis

Gd^{3+} concentrations (in millimoles per liter) were obtained from a representative macaque MR imaging study of the gravid uterus after maternal intravenous gadoteridol injection. In vivo measurements were obtained for 6 minutes after injection, by using

Figure 1

Figure 1: Sagittal T2-weighted half-Fourier rapid acquisition with relaxation enhancement MR image shows placement of three-dimensional ROI around a single in utero macaque fetus for in vivo quantification of Gd^{3+} concentration, as described by Schabel and Parker (28) and Schabel and Morrell (29).

regions of interest (ROIs) placed on the maternal kidney, maternal muscle, and the placenta and a three-dimensional ROI over the fetus (Fig 1). Relative enhancement was converted to Gd^{3+} concentration by using the full nonlinear signal equation described by Schabel and Parker (28), with field-dependent relaxivity values and preinjection values of T10 determined by using the variable flip angle method with flip angles of 3° and 25° (29,30).

Tissue Gd^{3+} Assay

Inductively coupled plasma mass spectrometry was performed to assess the amount of Gd^{3+} in the fetal tissues. The analysis was performed in the Elemental Analysis Core at Oregon Health and Science University by using an Agilent 7700× device equipped with an ASX 250 autosampler. For the analysis, tissue or fluid samples of approximately 100 mg were weighed and transferred into acid-treated borosilicate tubes and were digested with 1 mL concentrated HNO_3 (trace metal grade, Fisher Scientific, Pittsburgh, Pa) at 90°C for 2

hours. After digestion of the samples, 1 mL H_2O_2 (trace metal grade, Fisher Scientific) and 4 mL of 1% HNO_3 were added, and the samples were transferred into clean, acid-treated 15-mL conical tubes. For measurement, ×11 dilutions of samples were prepared in 1% HNO_3. Data were quantified by using a nine-point calibration curve (0, 0.5, 1, 2, 5, 10, 50, 100, and 1000 ppb [ng/g]) with external standards for Mn, Fe, Cu, Zn, and Gd (Common Elements Mix 2 Multi-Element Aqueous Standard and Gadolinium Single Elemental Standard; VHG Laboratories, Manchester, NH) in 1% HNO_3. For each sample, data were acquired in triplicate and were averaged. An internal standard (Internal Standard Multi-Element Mix 3; VHG Laboratories) introduced with the sample was used to correct for plasma instabilities, and frequent measurements of a 10-ppb all-analyte solution, as well as a blank (containing 1% HNO_3 only), were used as quality controls and to determine the coefficient of variance. To access the recovery rates of elements and to probe background contamination from containers, the following controls were treated, prepared, and analyzed by using the same method as the samples: certified National Institute of Standards and Technology standard reference material (bovine liver; 1577c), acid control (containing concentrated HNO_3 only), and certified elemental standards for inductively coupled plasma mass spectrometry (Common Elements Mix 2 Multi-Element Aqueous Standard and Gd^{3+} Single Elemental Standard; VHG Laboratories).

Note that inductively coupled plasma mass spectrometry is capable only of registering the presence of the Gd^{3+} ion; it is not possible to use it to distinguish between the chelated and dechelated forms of the ion. Accordingly, we use the term "Gd^{3+}" to refer to the presence of the gadolinium ion detected in the inductively coupled plasma mass spectrometry analysis, whether in the chelated state or in the dechelated form. The limit of detection for the samples was determined from calibration standards to be 0.6 parts per trillion, which resulted in a limit of detection of about 3.8×10^{-11} percent injected dose (ID) per gram.

Statistical Analysis

The quantitative levels of Gd^{3+} in the fetal tissue were expressed as percentages ID per gram or as percentages ID per organ. Percentage ID per gram reflects the percentage of the maternal ID found per gram of tissue. Percentage ID per organ represents the percentage of the injected maternal dose found in the organ of interest. For these calculations in amniotic fluid, the amniotic fluid volumes were estimated to be 80 mL, on the basis of limited normative values for the macaque and on our unpublished experience with approximate volumes of amniotic fluid removed and replaced during intrauterine surgeries in the gravid macaque (31). The Wilcoxon rank sum test, a nonparametric test, was used to compare the distributions of continuous variables between the high-fat and control groups and to compare the 19–21-hour group with the 45-hour group.

Results

Animals

Maternal weight ranged from 8.1 to 17.8 kg, with a mean of 12.6 kg. Fetal weight ranged from 211.3 to 434.8 g. Although altered placental function and placental inflammation have been reported in the diet-induced obesity model, the fetal and placental tissue concentrations of gadolinium chelate were evaluated as a group owing to small sample sizes (Table 1) (17,32).

Gd^{3+} Analysis

The in vivo Gd^{3+} concentrations in the maternal kidney, the maternal muscle, the placenta, and the entire fetus after maternal intravenous administration of gadoteridol indicated that the level of gadoteridol reaching the fetus was far lower than the level administered to the mother (Fig 2). As shown, the highest (95th percentile) of signal intensity measurements of Gd^{3+} in the fetus were still overall lower than the median concentrations of Gd^{3+} in the maternal kidney and muscle and in the placenta.

Quantitative amounts of Gd^{3+} in fetal tissue from the inductively coupled plasma mass spectrometry assay are provided in Tables 1 and 2. Table 3 shows comparative Gd^{3+} levels at the two time points. The median levels of Gd^{3+} in the amniotic fluid in the 45-hour group were significantly lower than those in the 19–21-hour group ($P = .01$). Amounts of gadolinium chelate were then expressed as percentages ID per gram of tissue and percentages ID per organ to assess the proportion of the maternal ID found in the fetal tissues (Tables 4, 5). In both the 19–21-hour group and the 45-hour group, the relative concentration (percentage ID per gram) was highest in the fetal kidneys (Fig 3). The highest total amount of Gd^{3+} was found in the amniotic fluid and placenta (percentage ID per organ) (Fig 4). A limited amount of Gd^{3+} was found in the liver, with very minimal to no Gd^{3+} found in the femur, skin, and brain.

Gd^{3+} levels in maternal plasma at the time of delivery showed trace levels of Gd^{3+} at 19–21 hours after injection (mean, $[2.5 \pm 1.3] \times 10^{-5}$ percent ID per gram), with the limit of detection of 3.8×10^{-11} percent ID per gram.

Discussion

We chose to utilize the contrast agent gadoteridol because of its inherent stability, which results from binding the gadolinium ion in a nonionic macrocyclic chelate (HP-DO3A). This stability would be expected to translate into minimal free ion disassociation and subsequently minimize the toxic effect of gadolinium. The Gd^{3+} chelates used for imaging vary in their thermodynamic and kinetic stability, with some much less likely to demetallate and release the toxic Gd^{3+} ion. The European Medicines Agency has categorized the various gadolinium agents as "highest risk," "intermediate risk," and "lowest risk" on the basis of the stability of the binding chelates (33). Because

Table 1

Quantitative Inductively Coupled Plasma Mass Spectrometry Measurements of Gd^{3+} in Fetal Tissues in the 19–21-hour Group

Organ or Tissue	Control Animals ($n = 3$)	Animals Receiving High-Fat Diet ($n = 8$)	*P* Value
Amniotic fluid	3.24 ± 0.50 (2.86–3.81)	3.28 ± 2.55 (1.21–9.15)	.47
Kidney	31.78 ± 9.55 (24.76–42.66)	32.38 ± 25.19 (12.24–87.11)	.61
Liver	2.49 ± 0.38 (2.20–2.92)	2.36 ± 0.96 (1.28–3.87)	.76
Brain	0.14 ± 0.20 (0.02–0.38)	0.16 ± 0.16 (0.014–0.40)	.92
Placenta	1.61 ± 0.29 (1.33–1.90)	1.67 ± 0.81 (0.68–2.82)	>.99
Skin*	0.72	1.0 ± 0.77 (0.45 And 1.54)	...
Femur*	0.38 (0.33–0.43) ± 0.07	0.43 ± 0.24 (0.22 And 0.76)	...

Note.—Data are mean measurements (in micrograms per gram) ± standard deviations, with ranges in parentheses. Data were obtained 19–21 hours after intravenous administration of a 0.1-mmol/kg dose of gadoteridol to the mother.

*For the skin and the femur, there was one animal in the control group and two animals in the high-fat diet group. *P* values were not calculated because of the small sample size.

Figure 2

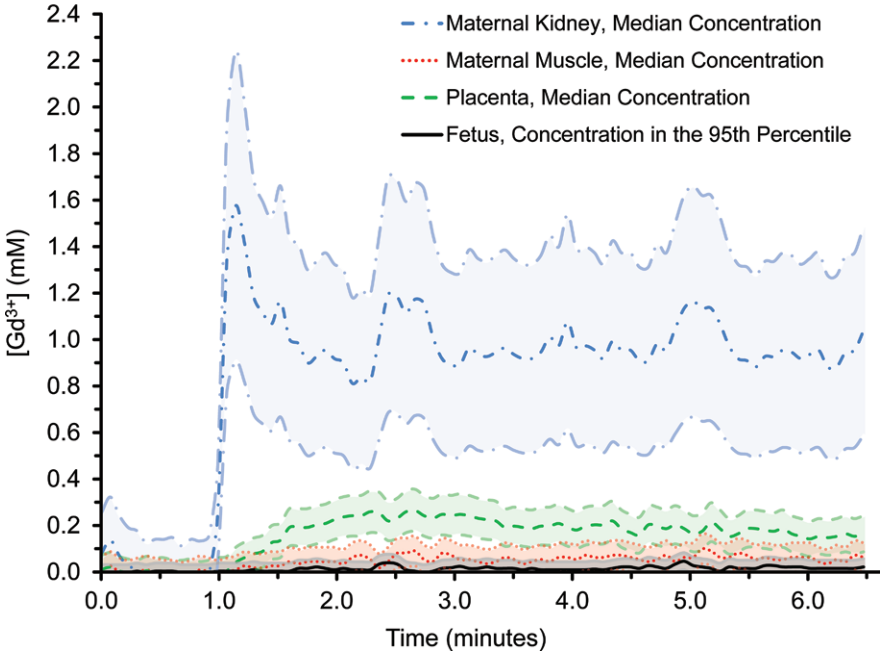

Figure 2: Graph shows in vivo Gd^{3+} concentration in maternal kidneys, maternal muscle, placenta, and the fetus versus time immediately after intravenous administration of 0.1 mmol/kg gadoteridol to the mother. The fetal concentration of Gd^{3+} is reported at the 95th percentile of the signal intensity measurements obtained from the three-dimensional ROI over the fetus, as compared with the median (substantially higher) concentrations in the maternal tissues. These data were obtained from a single representative gravid macaque after contrast agent injection. At time point 0.0, there is apparent detection of gadolinium chelate in the maternal kidney. This is likely an artifact due to respiratory motion. Shaded areas = standard deviations of the concentrations.

gadoteridol is in the lowest-risk category for nephrogenic systemic fibrosis, the European Society of Urogenital Radiology suggests that gadoteridol can be used to obtain essential diagnostic information in pregnancy (12).

We found that the overall amounts of Gd^{3+} in the fetal tissues and amniotic fluid are minimal, even 19–21 hours after maternal intravenous injection. In animal and human studies involving MR imaging after maternal injection, Gd^{3+}-based contrast agents have been shown to enhance the placenta (3), and transplacental transfer of these agents occurs (3,13,15,16). We theorized that likely only a small amount of the contrast agent reaches the fetal circulation; however, the percentage of the total dose of gadoteridol that actually crosses into the fetal circulation is unknown in primates. To gauge the relative in vivo amounts of contrast agent reaching the fetus compared with the maternal circulation immediately after intravenous gadoteridol injection, we estimated the amount of Gd^{3+} in the maternal kidney, maternal muscle, placenta, and fetus by measuring ROIs over these areas on dynamic MR images. As shown, the amount of gadoteridol reaching the fetus is far lower than that administered to the mother.

Japanese macaques have a developmental ontogeny that is similar to that in humans, including placental function (34,35). Like humans, nonhuman primates have a hemochorial placenta with organization into multiple cotyledons (36,37). Maternal blood flow is delivered to the placenta via the uterine arteries, which branch into spiral arteries and perfuse the intervillous space of the cotyledons of the placenta (38). Other researchers (13–15,39) have reported biodistribution in mice, rats, and rabbits; however, hemochorial placental organization is absent in these animals, which lack the nutrient exchange mechanism provided by the intervillous space.

Once gadoteridol is injected intravenously and enters the intervillous space of the placenta, the agent must transport through the trophoblast layers, which surround the fetal capillaries, into the fetal endothelial cells. Gaining access to the fetal vasculature, the gadoteridol then enters the fetal circulation via the umbilical vein, which delivers blood to the fetal heart after shunting it past the fetal liver via the ductus venosus. Subsequently, the agent is excreted by the fetal kidneys into the amniotic fluid

Table 2

Quantitative Inductively Coupled Plasma Mass Spectrometry Measurements of Gd^{3+} in Fetal Tissues in the 45-hour Group

Organ or Tissue	Control Animals ($n = 2$)	Animal Receiving High-Fat Diet ($n = 1$)
Amniotic fluid	0.28, 0.58	0.37
Kidney	10.41, 23.56	30.08
Liver	0.93, 2.07	3.96
Brain	0.04, 0.10	0.04
Placenta	0.60, 1.07	2.14

Note.—Data are micrograms per gram. Means and *P* values were not calculated because of the small sample size. Data were obtained 45 hours after intravenous administration of a 0.1-mmol/kg dose of gadoteridol to the mother.

Table 3

Gd^{3+} Levels in Fetal Tissues in the 19–21-hour Group and the 45-hour Group

Organ or Tissue	19–21-hour Group ($n = 11$)	45-hour Group ($n = 3$)	*P* Value
Amniotic fluid	2.86 ± 2.15 (1.21–9.15)	0.37 ± 0.15 (0.28–0.58)	.01
Kidney	27.64 ± 21.50 (12.24–87.11)	30.08 ± 12.33 (10.41–33.11)	>.99
Liver	2.34 ± 0.82 (1.28–3.87)	2.07 ± 1.53 (0.93–3.96)	.76
Brain	0.03 ± 0.16 (0.01–0.40)	0.04 ± 0.04 (0.04–0.10)	.88
Placenta	1.58 ± 0.69 (0.68–2.82)	1.07 ± 0.79 (0.60–2.14)	.35

Note.—Data are median gadolinium chelate concentrations in micrograms per gram of tissue ± standard deviations, with ranges in parentheses.

Table 4

Distribution of Gd^{3+} Ion in the Fetus 19–21 Hours after Maternal Gadoteridol Administration

Organ or Tissue	Percentage ID per Gram of Tissue	Percentage ID per Organ
Amniotic fluid	0.0017 ± 0.001	0.1361 ± 0.076
Kidney	0.0161 ± 0.008	0.0198 ± 0.0097
Liver	0.0013 ± 0.0004	0.0126 ± 0.0054
Brain	0.0001 ± 0.00007	0.0034 ± 0.0034
Placenta	0.0009 ± 0.0004	0.0939 ± 0.0494
Skin	0.0009 ± 0.0002	0.0008 ± 0.0005
Femur	0.0003 ± 0.0001	...

Note.—Data are means ± standard deviations. Data were obtained 19–21 hours after intravenous administration of a 0.1-mmol/kg dose of gadoteridol to the mother.

(13,16). Recirculation occurs when the gadoteridol is excreted into the amniotic fluid as urine, which the fetus regularly swallows during gestation (40,41). Solutes such as gadoteridol would presumably then be absorbed through the fetal gastrointestinal tract back into the fetal bloodstream. A small component of amniotic fluid volume results from fetal lung excretion as well (40). However, there are pathways through which gadoteridol may return to the maternal circulation. First, some of the agent can be sent back to the placenta via the umbilical arteries, which carry blood away from the fetus. Second, there can be intramembranous transport across the placental amnion into fetal microvessels at the fetal surface of the placenta (42). Gaining access to the fetal circulation through this mechanism of bulk flow, the agent can potentially cross back to the maternal circulation through the placenta.

Prolonged in vivo residence increases the risk of disassociation of the Gd^{3+} ion from its chelate (39,43,44). Liberated Gd^{3+} ion is toxic and could be detrimental to fetal development. Rapid clearance is therefore highly advantageous in ensuring that the chances of substantial dechelated Gd^{3+} accumulation within the fetoplacental circulation are minimized.

We quantified the amounts of Gd^{3+} in the nonhuman primate fetus, placenta, and amniotic fluid. Results of other studies (13–15,39) have shown biodistribution in gravid mice, rats, and rabbits after injection of variable doses of gadolinium contrast agents. In animal and human studies involving MR imaging after maternal injection, Gd^{3+}-based contrast agents have been shown to enhance the placenta (3), and transplacental transfer of these agents occurs (3,13,15,16). In our nonhuman primate model, the majority of Gd^{3+} was found in the amniotic fluid and placenta. This is consistent with perfusion of the placenta via the uterine arteries, passing a portion of the maternal dose of gadolinium-based contrast agents to the placenta. Once within the placental vascular system, Gd^{3+} in the fetal tissues and amniotic fluid reflects transplacental entrance into fetal circulation.

Gadoteridol is known to be excreted exclusively though the kidneys (39). As the contrast agent is filtered from the blood, the agent rapidly accumulates in the kidneys. Elevated levels of Gd^{3+} persist as excretion continues in adult rats after the injection of a weight-appropriate dose, and detectable levels of Gd^{3+} are found in the kidneys even 24 hours after injection (0.32% ID per gram) (39). Likewise, our results show a relatively greater concentration of Gd^{3+} in the fetal renal tissue, as expected owing to renal excretion. No published adult primate biodistribution data are

Table 5

Distribution of Gd^{3+} Ion in the Fetus 45 Hours after Maternal Gadoteridol Administration

Organ or Tissue	Percentage ID per Gram of Tissue	Percentage ID per Organ
Amniotic fluid	0.0007 ± 0.0009	0.0598 ± 0.0741
Kidney	0.0125 ± 0.0072	0.0163 ± 0.0084
Liver	0.0013 ± 0.0008	0.0126 ± 0.0071
Brain	0.00002 ± 0.00001	0.0014 ± 0.0008
Placenta	0.0008 ± 0.0005	0.0899 ± 0.0544

Note.—Data are means ± standard deviations. Data were obtained 45 hours after intravenous administration of a 0.1-mmol/kg dose of gadoteridol to the mother.

Figure 3

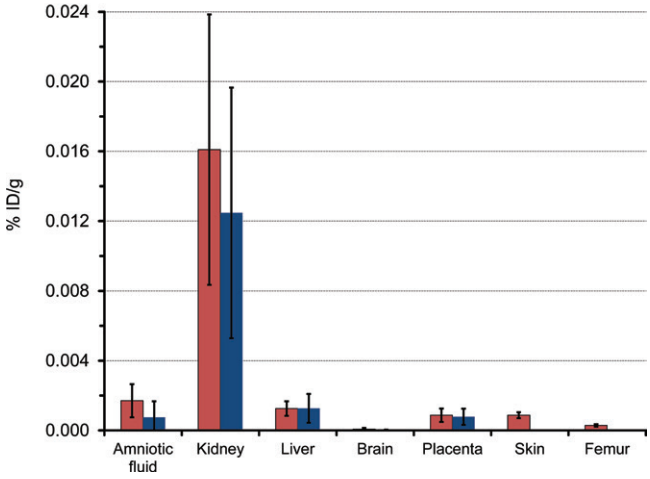

Figure 3: Bar graph shows distribution of Gd^{3+} in various fetal tissues of Japanese macaques 19–21 hours (red) and 45 hours (blue) after maternal injection of 0.1 mmol/kg of gadoteridol. Percentage ID per gram describes the relative concentration of the Gd^{3+} ion in the organ sampled. Error bars = first standard deviation.

available for comparative purposes, but these findings are consistent with rapid renal clearance of gadoteridol, intact, by the fetus. Fetal biodistribution data collected 45 hours after injection suggest that the gadoteridol continues to clear from the fetus. Although fetal levels of Gd^{3+} are already very low 19–21 hours after injection, amniotic fluid levels continue to decrease over time ($P < .05$). The small numbers in the delayed group did not allow determination of statistical significance in the fetal tissue levels; however, the values do not appear to be substantially increasing while amniotic fluid levels decrease. This suggests that the low levels of Gd^{3+} after injection are not simply the result of gadoteridol being excluded from the fetal circulation but that Gd^{3+} is also actively eliminated from the fetus.

Relatively little Gd^{3+} was observed in the fetal liver or femur tissues. Excretion through the hepatobiliary system would be expected to give rise to elevated levels of Gd^{3+} in the liver; however, both the concentration and the total Gd^{3+} level in the liver were found to be low—much lower than in adult rodents (39). Furthermore, the presence of minimal Gd^{3+} in the liver and femur strongly indicates that gadoteridol is excreted intact. If the Gd^{3+} ion dissociates from the chelate, it rapidly precipitates into particulate matter and is deposited in the reticuloendothelial system (the liver) and, eventually, in calcium-containing structures (39,45,46). The Gd^{3+} ion has comparable chemical properties to the Ca^{2+} ion and therefore in vivo has a high affinity for the phosphate ion. On the basis of results of rodent studies, dechelated Gd^{3+} deposits in the skeletal system within 1 day after injection (39,45,46). The minimal levels of Gd^{3+} observed in the fetal liver and femur in our study confirm negligible free ion deposition, as also observed in adult rodents (39,45,46).

We quantified Gd^{3+} in nonhuman primate fetal tissues after a weight-appropriate maternal dose and showed that the fate of gadoteridol entering the fetal circulation is very similar to that in the adult animal. As with human adults, there is no indication that the agent crosses the blood-brain barrier—the minute amounts detected are likely due to contamination from vascular structures. Trace amounts of the maternal dose were present in the highest-yield fetal tissues outside the kidneys (liver, bone, skin), similar to findings in adult animal models. No direct assessment of gadoteridol accumulation in maternal tissues was performed as part of our study because the necessary tissue samples were not available. Instead, Gd^{3+} levels in maternal plasma at the time of delivery were assessed and showed extremely low levels of Gd^{3+} ($[2.5 \pm 1.3] \times 10^{-5}$ percent ID per gram). These data are consistent with those in a previous report by Tweedle et al (39) of Gd^{3+} levels in adult rodents 24 hours after administration. Of note, the limit of detection for inductively coupled plasma mass spectrometry is far lower than the limit of detection for scintillation (3.8×10^{-11} percent ID per gram vs 0.004% ID per gram ± 0.001, respectively), which was the method used for quantification in that study (39). Additional studies could be performed to correlate the fetoplacental tissue levels of gadoteridol with the maternal tissue levels, to assess if maternal variations can alter fetal exposure to the agent.

Figure 4

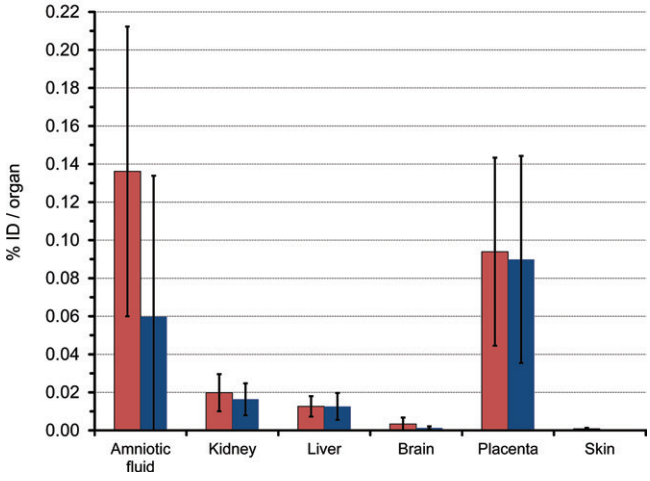

Figure 4: Bar graph shows distribution of Gd^{3+} in various fetal tissues of Japanese macaques 19–21 hours (red) and 45 hours (blue) after maternal injection of 0.1 mmol/kg of gadoteridol. Percentage ID per organ describes which samples contain the majority of residual Gd^{3+} ions. Error bars = first standard deviation.

Currently, opportunities for the use of Gd^{3+}-based contrast agents in the evaluation of the placenta include MR imaging of placental perfusion and enhancement in the setting of insufficiency or intrauterine growth restriction and, potentially, MR imaging of the morbidly adherent placenta. In the incidentally pregnant patient with abdominal pain, contrast media may be useful in the evaluation of acute appendicitis, pyelonephritis, inflammatory bowel disease, and neoplasm staging (8,10,47). In certain scenarios, the trace amount of residual Gd^{3+} in the fetoplacental circulation found in our study may be less clinically important than the diagnostic limitations existing when imaging without contrast material.

Practical application: Our study of the gravid nonhuman primate shows minimal residual Gd^{3+} in the fetal tissues and amniotic fluid by 21 hours after maternal intravenous injection of weight-based clinical doses of gadoteridol in the 3rd trimester, with the suggestion of continued excretion. Although there will likely be continued debate as to whether gadolinium chelate administration during pregnancy is justified for diagnostic imaging, our study provides information that may alleviate some uncertainty regarding the potential for Gd^{3+} toxicity to the fetus after maternal dosing.

Acknowledgments: We thank Megan Duffy, BA, in the Oregon Health and Science University Elemental Analysis Core for sample preparation, measurement, and data analysis, as well as for contributing the inductively coupled plasma mass spectrometry method to this report. Biostatistics support was provided by Yiyi Chen, PhD, as part of the Biostatistics Shared Resource of the Knight Cancer Institute.

Disclosures of Conflicts of Interest: K.Y.O. disclosed no relevant relationships. **V.H.J.R.** disclosed no relevant relationships. **M.C.S.** disclosed no relevant relationships. **K.L.G.** disclosed no relevant relationships. **M.W.** disclosed no relevant relationships. **A.E.F.** disclosed no relevant relationships.

References

1. Bardo D, Madriago E, Bohun C, et al. ECG-gating and MR fluoro in fetal cardiac MRI: preliminary results of with echo correlation. Presented at the 40th annual meeting of NASCI, Pasadena, CA, October 13–16, 2012.
2. Meoded A, Poretti A, Tekes A, Flammang A, Pryde S, Huisman TA. Prenatal MR diffusion tractography in a fetus with complete corpus callosum agenesis. Neuropediatrics 2011;42(3):122–123.
3. Frias AE, Schabel MC, Roberts VH, et al. Using dynamic contrast-enhanced MRI to quantitatively characterize maternal vascular organization in the primate placenta. Magn Reson Med 2014 Apr 18. doi: 10.1002/mrm.25264. [Epub ahead of print]
4. Palacios Jaraquemada JM, Bruno C. Gadolinium-enhanced MR imaging in the differential diagnosis of placenta accreta and placenta percreta. Radiology 2000;216(2):610–611.
5. Bardo D, Oto A. Magnetic resonance imaging for evaluation of the fetus and the placenta. Am J Perinatol 2008;25(9):591–599.
6. Warshak CR, Eskander R, Hull AD, et al. Accuracy of ultrasonography and magnetic resonance imaging in the diagnosis of placenta accreta. Obstet Gynecol 2006;108(3 Pt 1):573–581.
7. McLean LA, Heilbrun ME, Eller AG, Kennedy AM, Woodward PJ. Assessing the role of magnetic resonance imaging in the management of gravid patients at risk for placenta accreta. Acad Radiol 2011;18(9):1175–1180.
8. Leyendecker JR, Gorengaut V, Brown JJ. MR imaging of maternal diseases of the abdomen and pelvis during pregnancy and the immediate postpartum period. RadioGraphics 2004;24(5):1301–1316.
9. Pedrosa I, Zeikus EA, Levine D, Rofsky NM. MR imaging of acute right lower quadrant pain in pregnant and nonpregnant patients. RadioGraphics 2007;27(3):721–743; discussion 743–753.
10. Khandelwal A, Fasih N, Kielar A. Imaging of acute abdomen in pregnancy. Radiol Clin North Am 2013;51(6):1005–1022.
11. Tremblay E, Thérasse E, Thomassin-Naggara I, Trop I. Quality initiatives: guidelines for use of medical imaging during pregnancy and lactation. RadioGraphics 2012; 32(3):897–911.
12. ESUR Guidelines on Contrast Media, version 8.0. http:/www.esur.org/guidelines/. Accessed February 23, 2015.
13. Mühler MR, Clément O, Salomon LJ, et al. Maternofetal pharmacokinetics of a gadolinium chelate contrast agent in mice. Radiology 2011;258(2):455–460.
14. Okazaki O, Murayama N, Masubuchi N, Nomura H, Hakusui H. Placental transfer and milk secretion of gadodiamide injection in rats. Arzneimittelforschung 1996;46(1): 83–86.
15. Novak Z, Thurmond AS, Ross PL, Jones MK, Thornburg KL, Katzberg RW. Gadolinium-DTPA transplacental transfer and

distribution in fetal tissue in rabbits. Invest Radiol 1993;28(9):828–830.

16. Panigel M, Wolf G, Zeleznick A. Magnetic resonance imaging of the placenta in rhesus monkeys, Macaca mulatta. J Med Primatol 1988;17(1):3–18.
17. Frias AE, Morgan TK, Evans AE, et al. Maternal high-fat diet disturbs uteroplacental hemodynamics and increases the frequency of stillbirth in a nonhuman primate model of excess nutrition. Endocrinology 2011;152(6):2456–2464.
18. McCurdy CE, Bishop JM, Williams SM, et al. Maternal high-fat diet triggers lipotoxicity in the fetal livers of nonhuman primates. J Clin Invest 2009;119(2):323–335.
19. Aagaard-Tillery KM, Grove K, Bishop J, et al. Developmental origins of disease and determinants of chromatin structure: maternal diet modifies the primate fetal epigenome. J Mol Endocrinol 2008;41(2):91–102.
20. Comstock SM, Pound LD, Bishop JM, et al. High-fat diet consumption during pregnancy and the early post-natal period leads to decreased α cell plasticity in the nonhuman primate. Mol Metab 2012;2(1):10–22.
21. Sullivan EL, Grayson B, Takahashi D, et al. Chronic consumption of a high-fat diet during pregnancy causes perturbations in the serotonergic system and increased anxiety-like behavior in nonhuman primate offspring. J Neurosci 2010;30(10):3826–3830.
22. Sullivan EL, Smith MS, Grove KL. Perinatal exposure to high-fat diet programs energy balance, metabolism and behavior in adulthood. Neuroendocrinology 2011;93(1):1–8.
23. Suter M, Bocock P, Showalter L, et al. Epigenomics: maternal high-fat diet exposure in utero disrupts peripheral circadian gene expression in nonhuman primates. FASEB J 2011;25(2):714–726.
24. Suter MA, Chen A, Burdine MS, et al. A maternal high-fat diet modulates fetal SIRT1 histone and protein deacetylase activity in nonhuman primates. FASEB J 2012;26(12):5106–5114.
25. Grayson BE, Levasseur PR, Williams SM, Smith MS, Marks DL, Grove KL. Changes in melanocortin expression and inflammatory pathways in fetal offspring of nonhuman primates fed a high-fat diet. Endocrinology 2010;151(4):1622–1632.
26. Ma J, Prince AL, Bader D, et al. High-fat maternal diet during pregnancy persistently alters the offspring microbiome in a primate model. Nat Commun 2014;5:3889.
27. Pound LD, Comstock SM, Grove KL. Consumption of a Western-style diet during pregnancy impairs offspring islet vascularization in a Japanese macaque model. Am J Physiol Endocrinol Metab 2014;307(1):E115–E123.
28. Schabel MC, Parker DL. Uncertainty and bias in contrast concentration measurements using spoiled gradient echo pulse sequences. Phys Med Biol 2008;53(9):2345–2373.
29. Schabel MC, Morrell GR. Uncertainty in T(1) mapping using the variable flip angle method with two flip angles. Phys Med Biol 2009;54(1):N1–N8.
30. Rohrer M, Bauer H, Mintorovitch J, Requardt M, Weinmann HJ. Comparison of magnetic properties of MRI contrast media solutions at different magnetic field strengths. Invest Radiol 2005;40(11):715–724.
31. van Wagenen, Catchpole HR. Growth of the fetus and placenta of the monkey (Macaca mulatta). Am J Phys Anthropol 1965;23:22–33.
32. Roberts VH, Pound LD, Thorn SR, et al. Beneficial and cautionary outcomes of resveratrol supplementation in pregnant nonhuman primates. FASEB J 2014;28(6):2466–2477.
33. European Medicines Agency. Classification of gadolinium-containing contrast agents. http://www.ema.europa.eu/. Accessed September 25, 2014.
34. Ramsey EM, Houston ML, Harris JW. Interactions of the trophoblast and maternal tissues in three closely related primate species. Am J Obstet Gynecol 1976;124(6):647–652.
35. Myers RE. The gross pathology of the rhesus monkey placenta. J Reprod Med 1972;9(4):171–198.
36. Kaufmann P, Burton G. Anatomy and genesis of the placenta. In: Knobil E, Neill J, eds. The physiology of reproduction. 2nd ed. New York, NY: Raven, 1994.
37. Gruenwald P. Maternal blood supply to the coneptus. Eur J Obstet Gynecol Reprod Biol 1975;5(1-2):23–34.
38. Roberts VH, Räsänen JP, Novy MJ, et al. Restriction of placental vasculature in a nonhuman primate: a unique model to study placental plasticity. Placenta 2012;33(1):73–76.
39. Tweedle MF, Wedeking P, Kumar K. Biodistribution of radiolabeled, formulated gadopentetate, gadoteridol, gadoterate, and gadodiamide in mice and rats. Invest Radiol 1995;30(6):372–380.
40. Brans YW, Kuehl TJ, Hayashi RH, Andrew DS, Reyes P. Amniotic fluid in baboon pregnancies with normal versus growth-retarded fetuses. Am J Obstet Gynecol 1986;155(1):216–219.
41. Brans YW, Kuehl TJ, Hayashi RH, Shannon DL, Reyes P. Amniotic fluid composition in normal baboon pregnancies. J Reprod Med 1984;29(2):129–132.
42. Gilbert WM, Eby-Wilkens E, Tarantal AF. The missing link in rhesus monkey amniotic fluid volume regulation: intramembranous absorption. Obstet Gynecol 1997;89(3):462–465.
43. Allard M, Doucet D, Kien P, Bonnemain B, Caillé JM. Experimental study of DOTA-gadolinium: pharmacokinetics and pharmacologic properties. Invest Radiol 1988;23(Suppl 1):S271–S274.
44. Fogtmann M, Seshamani S, Kroenke C, et al. A unified approach to diffusion direction sensitive slice registration and 3-D DTI reconstruction from moving fetal brain anatomy. IEEE Trans Med Imaging 2014;33(2):272–289.
45. Wedeking P, Kumar K, Tweedle MF. Dose-dependent biodistribution of [153Gd] Gd(acetate)n in mice. Nucl Med Biol 1993;20(5):679–691.
46. Wedeking P, Tweedle M. Comparison of the biodistribution of 153Gd-labeled Gd(DTPA)2-, Gd(DOTA)-, and Gd(acetate)n in mice. Int J Rad Appl Instrum B 1988;15(4):395–402.
47. Katzberg RW, McGahan JP. Science to practice: will gadolinium-enhanced MR imaging be useful in assessment of at-risk pregnancies? Radiology 2011;258(2):325–326.